

MINIMAL OPTICAL COHERENCE TOMOGRAPHY B-SCAN DENSITY FOR RELIABLE DETECTION OF INTRARETINAL AND SUBRETINAL FLUID IN MACULAR DISEASES

PETRA P. FANG, MD, NIKLAS DOMDEI, MSc, PHILIPP HERRMANN, MD, PhD, FEBO, STEFFEN SCHMITZ-VALCKENBERG, MD, FEBO, FRANK G. HOLZ, MD, FEBO, WOLF M. HARMENING, PhD, TIM U. KROHNE, MD, FEBO

Purpose: To determine the minimal optical coherence tomography B-scan density for reliable detection of intraretinal and subretinal fluid.

Methods: Spectral domain optical coherence tomography raster scanning (Spectralis; Heidelberg Engineering, Heidelberg, Germany) using a scan field of $20^\circ \times 20^\circ$ of 97 B-scans with an interscan distance (ISD) of $60 \mu\text{m}$ was performed in 150 eyes of 150 consecutive patients at monitoring visits for intravitreal anti-vascular endothelial growth factor therapy. Using custom software, every other B-scan was repeatedly deleted to generate additional data sets with an ISD of $120 \mu\text{m}$ (49 B-scans), $240 \mu\text{m}$ (25 B-scans), and $480 \mu\text{m}$ (13 B-scans). Two independent reviewers evaluated the data sets for the presence of cystoid spaces of intraretinal fluid and subretinal fluid.

Results: Treatment diagnoses were neovascular age-related macular degeneration (68.0%), macular edema secondary to retinal vein occlusion (20.7%), diabetic macular edema (10.7%), and other retinal diseases (4.0%). Using the source data sets with an ISD of $60 \mu\text{m}$, intraretinal fluid was detected in 56.0%, subretinal fluid in 19.3%, and either/both in 68.7%. Compared with these results, the sensitivity of detection of intraretinal fluid and/or subretinal fluid using an ISD of $120 \mu\text{m}$, $240 \mu\text{m}$, and $480 \mu\text{m}$ was 99.0% (95% confidence interval, 94.7–100.0; $P = 0.5$), 97.1% (91.7–99.4; $P = 0.1$), and 87.4% (79.4–93.1; $P = 0.0001$), respectively.

Conclusion: An increase of ISD up to $240 \mu\text{m}$ does not significantly impair the detection of treatment-relevant exudative retinal changes in monitoring during intravitreal therapy of macular diseases. These findings are relevant for the choice of optical coherence tomography B-scan density in both routine clinical care and interventional clinical studies.

RETINA 0:1–7, 2017

Optical coherence tomography (OCT) is one of the most frequently used diagnostic techniques in today's clinical ophthalmology, mainly because of its pivotal role in the treatment monitoring of intravitreal therapies for macular diseases. Spectral domain OCT volume scans of the entire macular area represent the current standard for the detection of treatment-relevant exudative retinal changes such as intraretinal fluid (IRF) and subretinal fluid (SRF). These three-dimensional volume scans are interpolated from parallel two-dimensional OCT scans (B-scans).¹ Current OCT devices allow for adjustment of the density of

these B-scans by changing the interscan distance (ISD). Higher B-scan density results in a higher transverse resolution of the generated volume scan but also in a prolonged acquisition time with potential secondary effects such as declining fixation of the patient and reduced scan quality because of malfixation artifacts and tear film breakup. Furthermore, higher B-scan density increases the amount of image data generated and, thus, the required data storage volume, the time for electronic data transfer, and the time for data reviewing. Therefore, knowledge of the minimal B-scan density that allows for reliable detection of treatment-

relevant retinal changes would be desirable for clinical application in intravitreal therapy.

Previous studies investigated the effect of OCT B-scan density on retinal thickness measurement in patients with diabetic macular edema and neovascular age-related macular degeneration (nAMD).^{2,3} For the OCT devices used in these studies (Cirrus; Carl Zeiss Meditec, Jena, Germany: 3D OCT-2000; Topcon, Tokyo, Japan), an OCT B-scan density of 16 B-scans per 6 mm on the retina, equivalent to an ISD of 375 μm was reported to be sufficient for accurate assessment of overall retinal thickness in diabetic macular edema and neurosensory retinal thickness in nAMD, whereas an ISD of 188 μm was required for measuring thickness of subretinal hyper-reflective material in nAMD. Another study using a similar OCT device (3D OCT-1000; Topcon) evaluated the impact of scan density on the qualitative assessment of exudative retinal changes in nAMD.⁴ This study concludes that an ISD of 188 μm or below is required for accurate detection of IRF, SRF, and pigment epithelial detachment, whereas an ISD of 375 μm results in a significantly reduced sensitivity of detection. However, ISD values between 188 μm and 375 μm were not analyzed.

The OCT device used in our study (Spectralis; Heidelberg Engineering) allows for ISDs of 60 μm , 120 μm , or 240 μm . Using OCT volume scan data acquired in a routine clinical setting in consecutive patients undergoing intravitreal therapy for a variety of macular diseases, we analyzed the minimal necessary B-scan density for reliable detection of treatment-relevant retinal changes.

Patients and Methods

Data Collection

The study was approved by the institutional review board of the Medical Faculty of the University of Bonn

From the Department of Ophthalmology, University of Bonn, Bonn, Germany.

Supported by Ernst und Berta Grimmke Foundation (to P.P.F. and T.U.K.) and German Research Foundation (DFG), grant HA 5323/5-1 (to W.M.H.).

(F, financial research support; C, consultant, R, recipient of lecture fees or travel reimbursements): P. P. Fang and Novartis: F; S. Schmitz-Valckenberg and Alcon/Novartis: C, F, and R; Allergan: C and F; Bayer: F and R; Bioeq/Formycon: C and F; Carl Zeiss Meditec: F; CenterVue: F; Genentech/Roche: F and R; Heidelberg Engineering: F; Optos: F; F. G. Holz and Acucela: C and F; Allergan: F and R; Bayer: C, F, and R; Bioeq: C and F; Boehringer Ingelheim: C; Carl Zeiss Meditec: F and R; Genentech: C, F, and R; Heidelberg Engineering: C, F, and R; Merz: C and F; NightstarX: F; Novartis: C, F, and R; Optos: F; Pixium: F; Roche: C and F; Thea: C; T. U. Krohne and Alimera Sciences: C and R; Bayer: C and R; Heidelberg Engineering: R; Novartis: C, F, and R. The remaining authors have no financial/conflicting interests to disclose.

Reprint requests: Tim U. Krohne, MD, FEBO, Department of Ophthalmology, University of Bonn, Ernst-Abbe-Street 2, 53127 Bonn, Germany; e-mail: krohne@uni-bonn.de

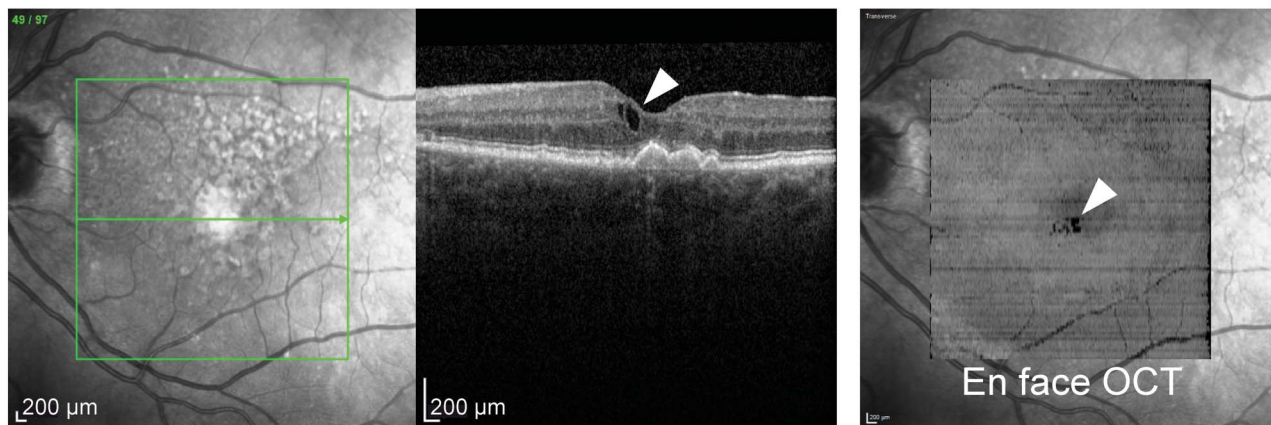
that waived the need for written patient consent because of the retrospective design of the study. We analyzed OCT volume scans that had been collected routinely from consecutive patients during monitoring visits for intravitreal anti-vascular endothelial growth factor therapy at the outpatient clinic of the Department of Ophthalmology, University of Bonn. All OCT scans were performed using the same OCT device (Spectralis; Heidelberg Engineering, Heidelberg, Germany) with identical settings, that is, a scan field of $20^\circ \times 20^\circ$ centered on the fovea, an ISD of 60 μm (97 B-scans), and real-time eye tracking with an averaging of at least 9 single frames per B-scan.

Image Analysis

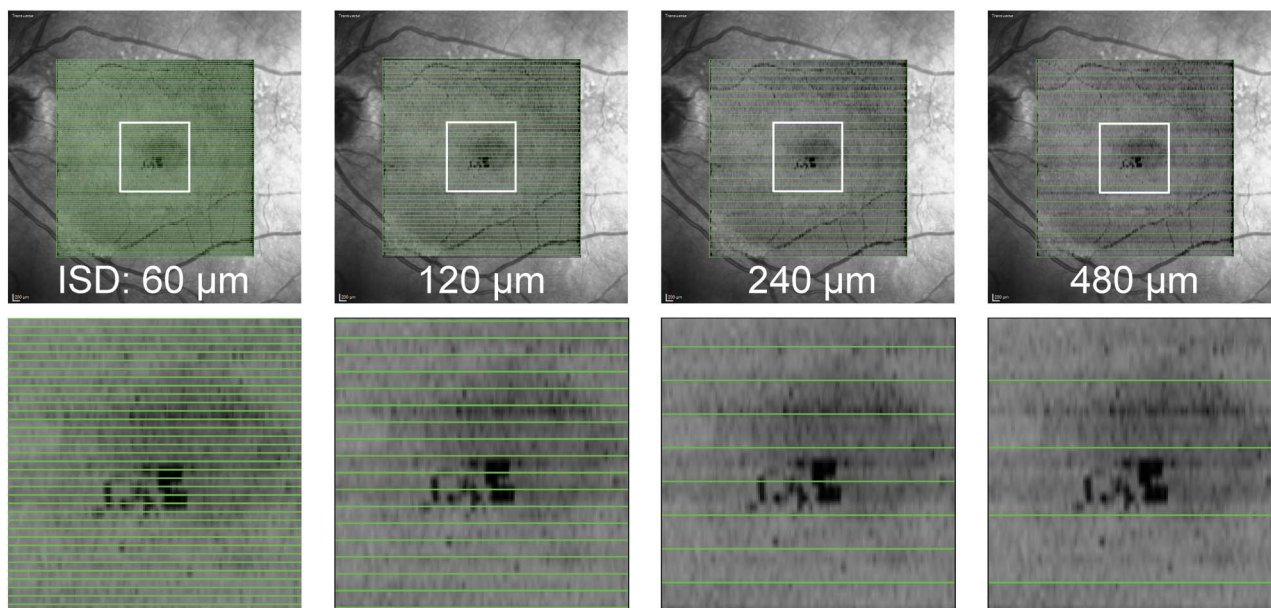
The OCT device used allows for adjustment of B-scan density to an ISD of 60 μm , 120 μm , and 240 μm . For comparison of OCT volume scans of different ISD, we sought to exclude differences between volume scans by possible misalignment. Therefore, we generated all volume scan data sets per patient from the same source data. For this, patients were imaged using the highest OCT B-scan density (ISD of 60 μm , total of 97 B-scans, equivalent to a B-scan density of 4.8 scans/degree) to create a baseline data set. Subsequently, we used custom software (Matlab; MathWorks, Natick, MA) to generate volume scans with reduced B-scan densities by repeatedly deleting every other B-scan from the original data sets (Figure 1). This resulted in additional data sets with an ISD of 120 μm (total of 49 B-scans, equivalent to a B-scan density of 2.4 B-scans/degree), 240 μm (25 B-scans, 1.2 B-scans/degree), and 480 μm (13 B-scans, 0.6 B-scans/degree). In addition, a single central B-scan was extracted from the baseline data sets. Two independent reviewers (T.U.K and P.H.) evaluated each of the resulting five OCT data sets per patient for the presence of cystoid spaces of IRF and SRF. Each patient's OCT scans were assessed in order of B-scan density starting with the least dense one. Thus, the readers were masked for the dense scans when evaluating the less dense ones. Interrater agreement was 95.9% for the detection of IRF and 98.1% for the detection of SRF. For statistical analysis, discrepant decisions were resolved by open discussion.

Statistical Analysis and Geometrical Model of Lesion Detection

Statistical analyses were performed using appropriate software (Excel 2013; Microsoft, Redmond, WA; GraphPad InStat 3.06; GraphPad Software, San Diego, CA). For the calculation of significance levels, we



A



B

Fig. 1. Illustration of the ISD parameters investigated. **A.** An exemplary study patient with nAMD exhibits IRF (white arrowhead) in OCT volume scan covering a retinal area of 20° by 20° (green arrow: location of single B-scan). En face OCT presentation of the data set demonstrates the dimensions of the IRF accumulation (white arrowhead). **B.** The en face OCT image of the IRF accumulation is overlaid by volume scan patterns of decreasing B-scan density as investigated in this study, equivalent to an ISD of $60\ \mu\text{m}$, $120\ \mu\text{m}$, $240\ \mu\text{m}$, and $480\ \mu\text{m}$.

used McNemar exact test. P values of less than 0.05 were considered statistically significant.

To theoretically support our experimental findings on the minimal ISD required for reliable detection of IRF and SRF, we used a geometrical model to estimate the probability with which lesions manifest as a detectable signal in the OCT image. Under some pragmatic optical simplification, we treated a single OCT B-scan as a cross-sectional cut of the retinal tissue with neglectable thickness. We defined the probability that any lesion is captured, P_c , by at least 1 B-scan as simply the fraction of the effective orthogonal extent of the lesion, d_{eff} , divided by ISD:

$$P_c(d, \text{ISD}) = \frac{d_{\text{eff}}}{\text{ISD}}, \quad (1)$$

with $P_c = 1$ if $d_{\text{eff}} \geq \text{ISD}$.

If a retinal lesion is captured in the image of 1 OCT B-scan, detection of that lesion by a human observer also depends on its image size and orientation. Using a device with a digital transverse resolution of $11\ \mu\text{m}$,⁵ we conservatively set the minimal detectable extent in a retinal OCT B-scan to be $50\ \mu\text{m}$. Assuming that retinal lesions have a spherical geometry, the effective one-dimensional extent, d_{eff} , depends on their diameter, d , by:

$$d_{\text{eff}} = \sqrt{(d^2 - 50\mu\text{m}^2)}, \quad (2)$$

thus, $P_c = 0$ if $d \leq 50 \mu\text{m}$.

Given multiple ISDs, we solved Equation 1 to find the values for d at which P_c becomes significantly large (greater than 0.9). If the diameter of retinal structures to be detected is known, Equation 1 can be used to generalize for the detection of any spherical retinal lesions.

Results

A total of 150 eyes of 150 consecutive patients (mean age, 77.3 ± 10.6 years) were included in the study. All eyes were under ongoing anti-vascular endothelial growth factor therapy (bevacizumab, ranibizumab, or aflibercept) using either a treat-and-extend regimen (98 eyes, 65.3%) or a pro re nata regimen (52 eyes, 34.7%), the latter mostly in bilaterally treated patients. Treatment diagnoses were nAMD (102 eyes, 68.0%), macular edema secondary to branch retinal vein occlusion (16 eyes, 10.7%), macular edema secondary to central retinal vein occlusion (15 eyes, 10.0%), diabetic macular edema (11 eyes, 10.7%), choroidal neovascularization secondary to pathological myopia (3 eyes, 2.0%), choroidal neovascularization secondary to central serous chorioretinopathy (2 eyes, 1.3%), and choroidal neovascularization secondary to pseudoxanthoma elasticum (1 eye, 0.7%).

Two independent reviewers evaluated the OCT volume scan data of the 150 included eyes for the presence of cystoid spaces of IRF and SRF (Table 1). In the source data sets with an ISD of $60 \mu\text{m}$, IRF was detected in 84 eyes (56.0%), SRF in 29 eyes (19.3%), and either or both in 103 eyes (68.7%). With increasing ISD, these detection rates decreased progressively. Intraretinal fluid and/or SRF were detected in 102 eyes (68.0%) using an ISD of $120 \mu\text{m}$, in 100 eyes (66.7%) using an ISD of $240 \mu\text{m}$, in 90 eyes (60.0%) using an ISD of $480 \mu\text{m}$, and in 58 eyes (38.7%) using a single central B-scan.

Considering the detection results for $60\text{-}\mu\text{m}$ ISD the ground truth, we calculated sensitivity and negative

predictive value of detection of IRF, SRF, and either/both for increasing ISD values (Table 2, Figure 2). The sensitivity of detection of IRF and/or SRF was 99.0% (95% confidence interval, 94.7–100.0) for $120\text{-}\mu\text{m}$ ISD, 97.1% (91.7–99.4) for $240\text{-}\mu\text{m}$ ISD, 87.4% (79.4–93.1) for $480\text{-}\mu\text{m}$ ISD, and 56.3% (46.1–66.1) for a single central B-scan. The respective negative predictive values were 97.9% (88.9–100.0), 94.0% (83.4–98.7), 78.3% (65.8–87.9), and 51.1% (40.5–61.6). Because of the study design with all data sets of each patient being generated from the same source data, specificity and positive predictive value were 100% for all ISD groups.

Compared with the results for $60\text{-}\mu\text{m}$ ISD, a statistically significant reduction of sensitivity of detection of IRF and/or SRF was only found for $480\text{-}\mu\text{m}$ ISD ($P = 0.0001$) and the single central B-scan ($P < 0.0001$) but not for $120\text{-}\mu\text{m}$ ISD ($P = 0.5$) and $240\text{-}\mu\text{m}$ ISD ($P = 0.1$). Furthermore, a sensitivity of detection of above 90% that has previously been used as a criterion for sufficient B-scan density⁴ was reached for ISDs up to $240 \mu\text{m}$ but not for $480\text{-}\mu\text{m}$ ISD or the single central B-scan. Both results consistently indicate that an increase of ISD up to $240 \mu\text{m}$ does not result in a significant impairment of the detection of IRF and SRF.

Geometrical modeling determined the theoretical lower size limit for lesions that can be reliably detected (probability $\geq 90\%$) using an ISD of $60 \mu\text{m}$, $120 \mu\text{m}$, $240 \mu\text{m}$, and $480 \mu\text{m}$ to be $74 \mu\text{m}$, $119 \mu\text{m}$, $222 \mu\text{m}$, and $435 \mu\text{m}$, respectively, whereas lesions below these size limits may be missed by OCT scans of the respective ISD. Clinical examples illustrating the size of actual retinal lesions that were detected or missed using different ISDs are provided (Figure 3).

Discussion

This retrospective cross-sectional study determined the minimal OCT B-scan density for reliable detection of exudative retinal alterations, using an OCT device that uses B-scan densities equivalent to an ISD of $60 \mu\text{m}$, $120 \mu\text{m}$, and $240 \mu\text{m}$. Our results indicate that an increase of ISD from $60 \mu\text{m}$ up to $240 \mu\text{m}$ does not result in a significantly decreased detection rate for IRF and SRF. These findings have implications for

Table 1. Detection of IRF and SRF in the Study Cohort of 150 Eyes Using Different ISDs or a Single Central B Scan

	60- μm ISD (%)	120- μm ISD (%)	240- μm ISD (%)	480- μm ISD (%)	Single B Scan (%)
IRF	84 (56.0)	83 (55.3)	81 (54.0)	71 (47.3)	45 (30.0)
SRF	29 (19.3)	29 (19.3)	29 (19.3)	26 (17.3)	16 (10.7)
IRF and/or SRF	103 (68.7)	102 (68.0)	100 (66.7)	90 (60.0)	58 (38.7)

Data represent the number of eyes and percentage of total eyes.

Table 2. Sensitivity and Negative Predictive Value (NPV) for the Detection of IRF and SRF Using Different ISDs or a Single Central B Scan as Compared to an ISD of 60 μm

	120- μm ISD	240- μm ISD	480- μm ISD	Single B Scan
IRF				
Sensitivity (95% CI)	98.8% (93.6–100.0)	96.4% (89.9–99.3)	84.5% (75.0–91.5)	53.6% (42.4–64.5)
NPV (95% CI)	98.5% (92.0–100.0)	95.7% (87.8–99.1)	83.5% (73.5–91.0)	62.9% (52.8–72.1)
Significance	$P = 0.5$ (n. s.)	$P = 0.1$ (n. s.)	$P = 0.0001$	$P < 0.0001$
SRF				
Sensitivity (95% CI)	100.0% (88.1–100.0)	100.0% (88.1–100.0)	89.7% (72.6–97.8)	55.2% (35.7–73.6)
NPV (95% CI)	100.0% (97.0–100.0)	100.0% (97.0–100.0)	97.6% (93.1–99.5)	90.3% (84.0–94.7)
Significance	$P = 1$ (n. s.)	$P = 1$ (n. s.)	$P = 0.1$ (n. s.)	$P = 0.0001$
IRF and/or SRF				
Sensitivity (95% CI)	99.0% (94.7–100.0)	97.1% (91.7–99.4)	87.4% (79.4–93.1)	56.3% (46.1–66.1)
NPV (95% CI)	97.9% (88.9–100.0)	94.0% (83.4–98.7)	78.3% (65.8–87.9)	51.1% (40.5–61.6)
Significance	$P = 0.5$ (n. s.)	$P = 0.1$ (n. s.)	$P = 0.0001$	$P < 0.0001$

CI, confidence interval; n. s., not significant.

OCT acquisition protocols in both routine clinical care and interventional clinical studies.

For the automated analysis of retinal and choroidal thickness by OCT volume scans, an ISD of 375 μm and 480 μm , respectively, has been reported as sufficient.^{2,3,6} The impact of OCT B-scan density on the qualitative assessment of retinal changes has been investigated by Baranano et al.⁴ The authors analyzed cystoid spaces of IRF, diffuse retinal thickening, SRF, pigment epithelial detachment, and subretinal tissue in patients with nAMD, using a different OCT device (3D OCT-1000; Topcon) compared with our study.⁴ They conclude that an ISD of 188 μm is sufficient for accurate detection, defined by a sensitivity of at least 90%, of most of these features, whereas sensitivity of detection was reduced in scans of 375- μm ISD. Inter-scan distance values between 188 μm and 375 μm , such as an ISD of 240 μm , were not analyzed.

For clinical routine, reducing OCT B-scan density yields several benefits including a shorter examination time.^{7,8} Especially in patients with poor fixation due to macular disease, higher scan densities result in a longer

acquisition time with possible secondary effects such as artifacts by malfixation and tear film breakup. Thus, a lower scan density and, therefore, shorter acquisition time would help to acquire more accurate volume scans in a clinically practical time frame.⁹ Although OCT acquisition time could also be reduced by measures such as minimizing the scan area or omitting the follow-up function, this is only feasible to a limited extent because sufficient scan area size and use of follow-up function are widely considered indispensable for intravitreal therapy monitoring.

A low B-scan density also allows for a higher number of single B-scans to be averaged in the same time and thus for increased signal-to-noise ratio. Avoidance of malfixation artifacts and increased image quality are expected to result in increased detection of pathological changes as well as improved automated segmentation and retinal thickness measurements.^{10,11} Furthermore, OCT volume scans of lower B-scan density also require less memory space and shorter processing time. In particular, in the setting of larger clinical centers and multicenter sites, this also

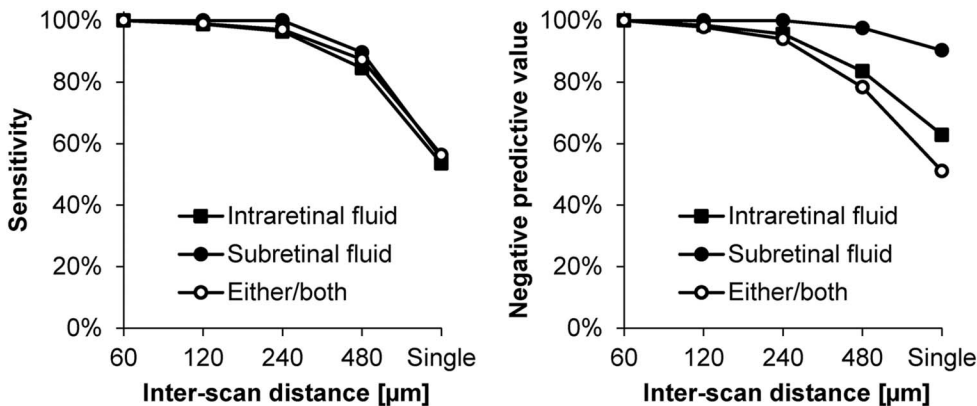


Fig. 2. Sensitivity and negative predictive value for the detection of IRF, SRF, or either/both. After OCT volume scan imaging with 60- μm ISD, data sets with reduced ISDs of 120 μm , 240 μm , and 480 μm were generated by deletion of alternating B-scans from the original data sets. In addition, the central B-scan was extracted as a single-line scan (single). Sensitivity and negative predictive value of detection of IRF, SRF, and either/both were calculated as compared to the results using an ISD of 60 μm . Only volume scans with an ISD of 480 μm

and single central B-scans exhibited a sensitivity of detection that was significantly reduced compared with the volume scans of 60- μm ISD.

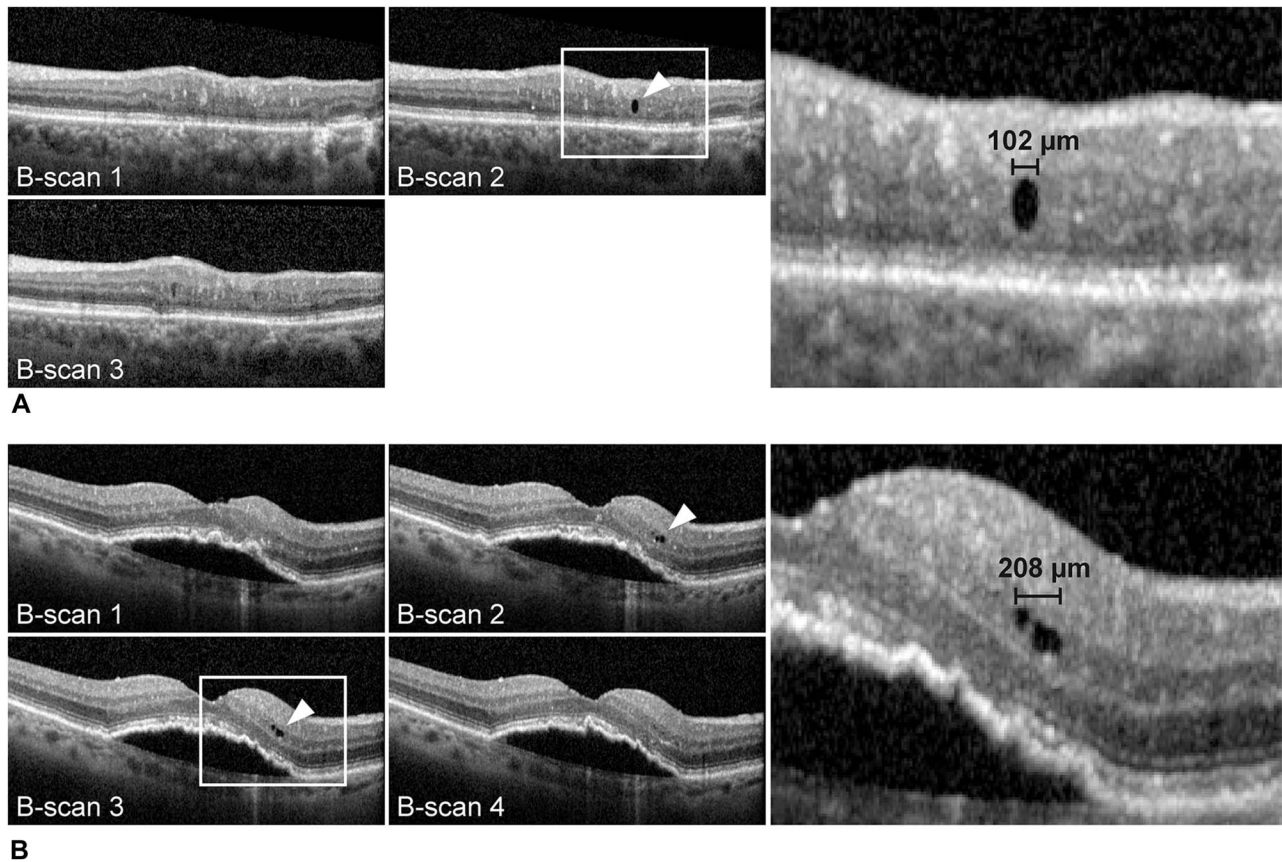


Fig. 3. **A.** Example of a retinal lesion $<120\ \mu\text{m}$ that can be missed when using OCT B-scans with an ISD of $120\ \mu\text{m}$. In 3 consecutive B-scans with $60\text{-}\mu\text{m}$ ISD, the lesion (white arrowhead) was detectable only in the middle B-scan 2. **B.** Example of lesion $<240\ \mu\text{m}$ that can be missed by a $240\text{-}\mu\text{m}$ ISD. In 4 consecutive B-scans with an ISD of $60\ \mu\text{m}$, the lesion (white arrowheads) was detectable only in the middle 2 B-scans 2 and 3.

reduces the data volume in the network and allows for faster electronic data transfer. About further evaluation and grading of OCT data, a reduced number of B-scans also facilitate manual correction of segmentation errors.^{12,13}

Our results indicate that an increase of ISD up to $240\ \mu\text{m}$ does not significantly impair the detection of treatment-relevant retinal changes during intravitreal anti-vascular endothelial growth factor therapy for macular diseases. Using a geometrical model, we determined the theoretical minimal lesion size that is reliably detected by this ISD to be $222\ \mu\text{m}$. Clinical examples from our study cohort demonstrating the size of actual retinal lesions that may potentially be missed with an ISD of $240\ \mu\text{m}$ are provided (Figure 3). Both the geometrical modeling results and the clinical example images illustrate that lesions need to be comparatively small and isolated to be at risk of being missed by an ISD of $240\ \mu\text{m}$. The therapeutic relevance of such lesions is unknown but seems to be questionable, thus supporting the suitability of OCT scans with $240\text{-}\mu\text{m}$ ISD in routine intravitreal treatment monitoring. However, longitudinal studies are

needed to provide data on the minimal size of retinal cystoid lesions that require treatment.

Our study investigated the impact of OCT scan density in the context of intravitreal treatment monitoring, thus focusing on IRF and SRF associated with exudative macular diseases. The results, thus, may not apply to the OCT analysis of other retinal diseases that may require higher OCT scan densities or different OCT scan patterns. For instance, for the assessment of localized foveal pathologies such as vitreomacular traction or macular hole, radial OCT scanning patterns have been shown to result in increased disease detection rates and may thus be preferable.^{14,15} For the detection of IRF and SRF in nAMD, however, a 12-line radial B-scan pattern was not found to be superior to a parallel B-scan pattern with an ISD of $240\ \mu\text{m}$.¹⁶

Our study has several limitations including its retrospective design, the use of only one OCT device, and the relative overrepresentation of nAMD in our study cohort. As the OCT device used in our study allows for B-scan densities up to an ISD of $60\ \mu\text{m}$, we had no means to assess whether we missed any retinal changes that would have been detectable by even

higher scan densities. Furthermore, because this study was performed as a cross-sectional analysis, the impact of OCT B-scan density on the results of anti-vascular endothelial growth factor therapy was not assessed. Because of the axial length, the central scan field of $20^\circ \times 20^\circ$ as used in our study is enlarged in axial myopes and reduced in axial hypermetropes leading to varying ISDs when using the same B-scan density in patients with different refractive errors. Especially in high myopic patients, this can impair the detection of subtle changes with high ISD and should be considered in clinical routine.

Moreover, our study focused on the detection of IRF and SRF only but did not take other structural changes into account such as subpigment epithelial fluid, retinal thickness, retinal pigment epithelial tears, atrophy, fibrosis, or retinal hemorrhage. For detection of these morphologic alterations, a multimodal imaging approach is recommended.^{17,18} Furthermore, monitoring during intravitreal therapy usually mandates repeated follow-up examinations. Current OCT technology allows for real-time eye tracking and automated positioning of follow-up B-scans at the same anatomical location. In addition to sufficient B-scan density, application of these technologies is considered an essential prerequisite for improving detection and reliable evaluation of retinal changes over time.^{19,20}

In conclusion, we found that in OCT volume scans, a B-scan density of 1.2 B-scans/degree, equivalent to an ISD of 240 μm , was sufficient for reliable detection of treatment-relevant retinal changes such as IRF and SRF during monitoring of intravitreal therapy in exudative macular diseases. These results have implications for the choice of OCT scan parameters in both routine clinical care and clinical trials.

Key words: optical coherence tomography, retinal imaging, image analysis, OCT B-scan density, macular diseases, age-related macular degeneration, diabetic macular edema, retinal vein occlusion, intravitreal injection, anti-vascular endothelial growth factor therapy.

References

- Drexler W, Fujimoto JG. State-of-the-art retinal optical coherence tomography. *Prog Retin Eye Res* 2008;27:45–88.
- Nittala MG, Konduru R, Ruiz-Garcia H, Sadda SR. Effect of OCT volume scan density on thickness measurements in diabetic macular edema. *Eye (Lond)* 2011;25:1347–1355.
- Velaga SB, Nittala MG, Konduru RK, et al. Impact of optical coherence tomography scanning density on quantitative analyses in neovascular age-related macular degeneration. *Eye (Lond)* 2017;31:53–61.
- Baranano AE, Keane PA, Ruiz-Garcia H, et al. Impact of scanning density on spectral domain optical coherence tomography assessments in neovascular age-related macular degeneration. *Acta Ophthalmol* 2012;90:e274–e280.
- Fleckenstein M, Charbel Issa P, Helb HM, et al. High-resolution spectral domain-OCT imaging in geographic atrophy associated with age-related macular degeneration. *Invest Ophthalmol Vis Sci* 2008;49:4137–4144.
- Chhablani J, Barteselli G, Bartsch DU, et al. Influence of scanning density on macular choroidal volume measurement using spectral-domain optical coherence tomography. *Graefes Arch Clin Exp Ophthalmol* 2013;251:1303–1309.
- Menke MN, Dabov S, Knecht P, Sturm V. Reproducibility of retinal thickness measurements in healthy subjects using spectralis optical coherence tomography. *Am J Ophthalmol* 2009;147:467–472.
- Courtney RJ, McClintic JI, Ehlers JP. Comparison of spectral domain optical coherence tomography scan patterns and clinical review strategies in neovascular age-related macular degeneration. *Retina* 2015;8:583–592.
- Sadda SR, Wu Z, Walsh AC, et al. Errors in retinal thickness measurements obtained by optical coherence tomography. *Ophthalmology* 2006;113:285–293.
- Giani A, Pellegrini M, Invernizzi A, et al. Aligning scan locations from consecutive spectral-domain optical coherence tomography examinations: a comparison among different strategies. *Invest Ophthalmol Vis Sci* 2012;53:7637–7643.
- Patel PJ, Chen FK, da Cruz L, Tufail A. Segmentation error in Stratus optical coherence tomography for neovascular age-related macular degeneration. *Invest Ophthalmol Vis Sci* 2009;50:399–404.
- Ghazi NG, Kirk T, Allam S, Yan G. Quantification of error in optical coherence tomography central macular thickness measurement in wet age-related macular degeneration. *Am J Ophthalmol* 2009;148:90–96.e2.
- Sadda SR, Keane PA, Ouyang Y, et al. Impact of scanning density on measurements from spectral domain optical coherence tomography. *Invest Ophthalmol Vis Sci* 2010;51:1071–1078.
- Schneider EW, Todorich B, Kelly MP, Mahmoud TH. Effect of optical coherence tomography scan pattern and density on the detection of full-thickness macular holes. *Am J Ophthalmol* 2014;157:978–984.e1.
- Rahimy E, Rayess N, Maguire JI, Hsu J. Radial versus raster spectral-domain optical coherence tomography scan patterns for detection of macular pathology. *Am J Ophthalmol* 2014;158:345–353.e2.
- Adam MK, Rayess N, Rahimy E, et al. Radial versus raster spectral-domain optical coherence tomography scan patterns for detection of macular fluid in neovascular age-related macular degeneration. *Br J Ophthalmol* 2016;100:491–494.
- Thiele S, Nadal J, Fleckenstein M, et al. Longitudinal analysis of drusen volume in intermediate age-related macular 2 degeneration using different SD-OCT scan patterns. submitted.
- Holz FG, Sadda SVR, Staurenghi G, et al. Imaging protocols in clinical studies in advanced age-related macular degeneration: recommendations from classification of atrophy consensus meetings. *Ophthalmology* 2017;124:464–478.
- Schmitz-Valckenberg S, Brinkmann CK, Fleckenstein M, et al. Fallstricke in der Netzhautbildgebung mittels optischer Kohärenztomographie [in German]. *Ophthalmologie* 2017;114:275–290.
- Heimes B, Schick T, Brinkmann CK, et al. Design des ORCA-Moduls der OCEAN-Studie: evaluierung der SD-OCT-Befunderhebung in der täglichen Praxisroutine [in German]. *Ophthalmologie* 2016;113:570–580.